



Grain refinement of Al–Si alloys by Nb–B inoculation. Part II: Application to commercial alloys



L. Bolzoni*, M. Nowak, N. Hari Babu

BCAST – (Brunel Centre for Advanced Solidification Technology), Brunel University, Uxbridge, Middlesex UB8 3PH, UK

ARTICLE INFO

Article history:

Received 15 July 2014

Accepted 21 August 2014

Available online 6 September 2014

Keywords:

Al alloys

Grain refinement mechanism

Heterogeneous nucleation

Solidification microstructure

Nb–B inoculation

ABSTRACT

The potency of Nb–B inoculation for the refinement of Al–Si cast alloy has been demonstrated in Part I of this work by the systematic analysis of binary Al–xSi alloys (where $x = 1–10$ wt.%). In Part II of this work the effect of Nb–B inoculation on commercial Al–Si alloys is assessed. Specifically, hypo-eutectic alloys such as LM24 (A380) and LM25 (A356) as well as near-eutectic LM6 (A413) Al–Si alloys are considered. The aim is to quantify the grain refinement and detect possible interaction with alloying elements commonly present in Al cast alloys, such as Mg, Fe, Cu, Mn and Zn. The in-depth analysis of the alloys solidified under wide range of cooling rates indicates that Nb–B inoculation does not only lead to a much finer microstructural features but also makes the final grain size far less sensitive to the cooling rate employed to solidify the material. Finally, the mechanism essential for the grain refinement of commercial Al cast alloys by Nb–B inoculation is determined on the base of SEM and thermal analysis results. It is found that in-situ formed Al_3Nb and NbB_2 intermetallic particles (forming from the interaction of Al alloy/Nb powder/ KBF_4 flux) are the heterogeneous nuclei responsible for the grain refining of Al cast alloys.

© 2014 Elsevier Ltd. All rights reserved.

1. Introduction

As discussed in Part I of this article, there is a great scientific interest in the development of efficient and reliable grain refiner for the Al industry because of the intrinsic advantages of finer microstructures [1–4]. Grain refinement is a common industrial practise for wrought Al [4–12] and it is mainly done by adding commercial master alloys. Modifications of the Al–Ti–B and Al–Ti–C master alloys have been recently investigated [13–17]. Commercial master alloys are not very effective on refining the most important Al casting alloys, i.e. the alloy based on the Al–Si system. The poor refinement is due to the interaction between Si and Ti which leads to the formation of titanium silicides depleting the melt of Ti. This phenomenon, which is called poisoning effect, is well known and was the subject of study of many researches [8,10,18–22]. Currently, the producers of Al cast part (e.g. automotive components manufacturers) do not use any grain refiner or employ the commercial Al–Ti–B master alloys even though of their poor performance. In Part I of this paper it has been demonstrated that Nb–B inoculation is able to refine the microstructural features, namely primary Al α -grains and Al–Si eutectic phase, of binary Al–xSi alloys (where $x = 1–10$ wt.%). Nevertheless, in that study

the following aspects were not considered: (1) can Nb–B inoculation effectively refine commercial Al–Si alloys where other alloying elements, rather than Si, are present? (2) is there any effect from the cooling rate used in the different casting techniques, i.e. sand casting, permanent mould casting and high-pressure die casting after Nb–B inoculation? (3) what is the impact of the finer microstructure of commercial Al–Si alloy on their mechanical performances? and (4) what is the nature of the particles responsible for the grain refining by Nb–B inoculation? These questions arise because commercial Al casting alloys are based on the Al–Si system due to their high fluidity but their composition, normally, contemplate other alloying elements in order to fulfil specific requirements. For examples, copper (1.5–4.5 wt.%) increases strength and improves machinability, nickel (0.3–2.3 wt.%) improves elevated temperature properties and magnesium (0.1–1.3 wt.%) enhance the corrosion resistance [23]. Moreover, the different commercial Al–Si alloys were designed to be processed by diverse solidification techniques which, in turns, result in different cooling rates. This is also the case of casting products with complex geometry where different wall thicknesses of the same product solidify under different cooling conditions. The experimental work discussed in this work was designed to answer the questions previously listed and, therefore, the applicability of Nb–B inoculation was tested in commercial Al–Si alloys considering a great range of cooling rates. The effect of the grain refinement on the

* Corresponding author.

E-mail address: leandro.bolzoni@brunel.ac.uk (L. Bolzoni).

mechanical properties was determined as well. Finally, the attention was focused on the identification of the inoculants (potential heterogeneous nucleation substrates) responsible for the grain refinement of Al–Si alloys by Nb–B inoculation.

2. Experimental procedure

For the purpose of this study commercial hypo-eutectic and near-eutectic alloys were considered and their compositions are reported in Table 1.

From Table 1, the main difference between the two hypo-eutectic alloys, LM24 and LM25, is the amount of alloying elements added because LM24 has much higher content of Fe, Cu and Zn than LM25. The starting material was placed into a clay-bonded graphite crucible and melted at 800 °C in a conventional electrical resistance heating elements furnace. A dwell time of 1 h was set to guarantee the homogenisation of the temperature inside the molten metal. Afterwards, the reference alloy was left to cool down to 740 °C (± 3 °C) and cast. In the case of the addition of the grain refiner, 0.1 wt.% of Nb powder ($< 45 \mu\text{m}$) and KBF_4 flux were added to the melt (0.1 wt.%). The TP-1 test (Standard Test Procedure for Aluminum Alloy Grain Refiners) of the Aluminum Association [24] was used because it permits to determine the effect of the heterogeneous nucleation induced by the addition of grain refiners. Furthermore, in order to simulate the cooling rates of various casting techniques employed in the Al industry, a wedge-shaped copper mould was used. Finally, for the study of the undercooling by means of thermal analysis [6,25–28], the molten metal was left to cool inside a glass-wool externally lined crucible (cooling rate of ~ 0.3 °C/s). Once cast, the samples were cut and their cross-sections prepared for metallographic analysis by using the classical route of grinding with 120–1200 SiC papers plus polishing with OPS solution was employed. Macroetched cross-section samples were etched by means of Tucker's solution (15 ml HF + 15 ml HNO_3 + 45 ml HCl + 25 ml H_2O) whereas for microstructural analysis the specimens were electropolished. In particular, the samples were immersed into the electrolyte (20 ml of perchloric acid (HClO_4) mixed with 80 ml of acetic acid) and a DC current of 30 V was applied during 2 min. The microstructural analysis was carried out with a Carl Zeiss Axioscope A1 optical microscope. The primary α -Al grain size and the Al–Si eutectic phase size were measured with the dedicated program from pictures taken at different position along the cross-section of the samples. Tensile samples were obtained by means of different techniques depending on the nature of the alloy. For the LM25 and LM6 alloys the tensile specimens were cast using a permanent steel mould and, afterwards, machined to specific dimensions (ASTM: E8). In the case of the LM24 and LM6 alloys, which have sufficiently high fluidity, tensile samples were obtained by means of the high pressure die casting (HPDC) method. Specifically, a LK[®] Machinery Co. Ltd. HPDC equipment with a diameter of the plunger of 60 mm, a maximum accelerating shot speed of 6.22 m/s and a maximum shot distance of 405 mm was used. The settings employed during the injection of the alloys were: die temperature of 180 °C, shot distance of 200 mm and trigger pressure of 70 bars. Tensile tests were performed on an Instron[®] 5569 universal testing machine

using a crosshead speed of 2 mm/min, equivalent to a strain rate of $1.33 \times 10^{-3} \text{ s}^{-1}$. A 25 mm gauge length external extensometer was used to record the elongation of the samples. Ultimate tensile strength and strain at fracture (mean values of, at least, four tested samples) were obtained directly from the dedicated program of the universal testing machine. Vickers hardness measurements were performed by means of a Vickers-Armstrongs Ltd. Hardness tester.

3. Results and discussion

3.1. Effect of Nb–B inoculation and pouring temperature on the microstructure of commercial Al–Si alloys

The first experiment carried out was the comparison between the effect of the addition of the novel grain refiner and the commercial Al–5Ti–1B master alloy to the alloys solidified using the TP-1 mould (cooling rate approximately 3.5 °C/s) and employing three different pouring temperatures in each case. Specifically, for the LM24 alloy the pouring temperature ranges between 610 °C and 650 °C, for the LM25 from 630 °C to 680 °C whilst for the LM6 from 630 °C to 670 °C. Representative examples of micrographs are presented in Fig. 1 where, for brevity, the micrographs of each alloy with different addition (i.e. reference, Al–5Ti–1B and Nb–B) poured from one specific temperature are reported.

From the plane polarised light micrographs of the LM24 alloy without the addition of any grain refiner (reference), it can be seen that the microstructure is mainly composed of quite fine primary α -Al dendrites homogeneously distributed (Fig. 1a). With the increment of the pouring temperature from 610 °C to 650 °C, the size of the primary dendrites increases due to higher undercooling that the alloy experiences. The increment was quantified by image analysis and it was found that the primary Al α -grain size increases linearly approximately from 530 μm to 640 μm (Fig. 1j). In the case of the employment of a commercial Al–5Ti–1B master alloy (Fig. 1b), the main microconstituent of the LM24 alloy is still primary α -Al dendrites whose size increases linearly from 450 μm to 610 μm . Thus, the addition of the commercial Al–5Ti–1B master alloy has some grain refinement effect on the LM24 alloy but the benefits decreases with the increment of the pouring temperature. The average grain size reduction by the addition of the Al–5Ti–1B master alloy to the LM24 alloy is about $10 \pm 5\%$. Finally, Nb–B inoculation leads to a further reduction of the primary α -Al dendrites in comparison to the commercial master alloy because the primary Al α -grain size ranges between 430 μm and 560 μm . Once again, there is an increment of the grain size of the LM24 alloy with the pouring temperature but this does not seem to be linear with the increment of the pouring temperature. After Nb–B inoculation (Fig. 1c), the LM24 alloy presents a grain size almost $18 \pm 4\%$ finer with respect to the reference material. The microconstituents of the LM25 alloy without any addition (reference) and poured at the lowest temperature considered (630 °C) are very fine primary α -Al dendrites of around 220 μm which gives the impression that the microstructure is composed of equiaxed grains (Fig. 1d). As in the case of the LM24 alloy, the increment of the pouring temperature leads to a significant increment of the size of the primary dendrites which reaches approximately 460 μm at 680 °C

Table 1
Chemical composition of the commercial Al–Si alloys considered in the study.

Alloy type	Element (wt.%)								
	Al	Si	Mg	Fe	Cu	Mn	Ni	Zn	Ti
LM24 (A380)	Bal.	8.5	0.13	1.2	3.37	0.19	0.04	1.36	0.04
LM25 (A356)	Bal.	6–8	0.3	0.5	0.003	0.005	–	0.003	0.11
LM6 (A413)	Bal.	10.0–11.0	0.3	0.6	0.01	0.5	0.1	0.1	0.1

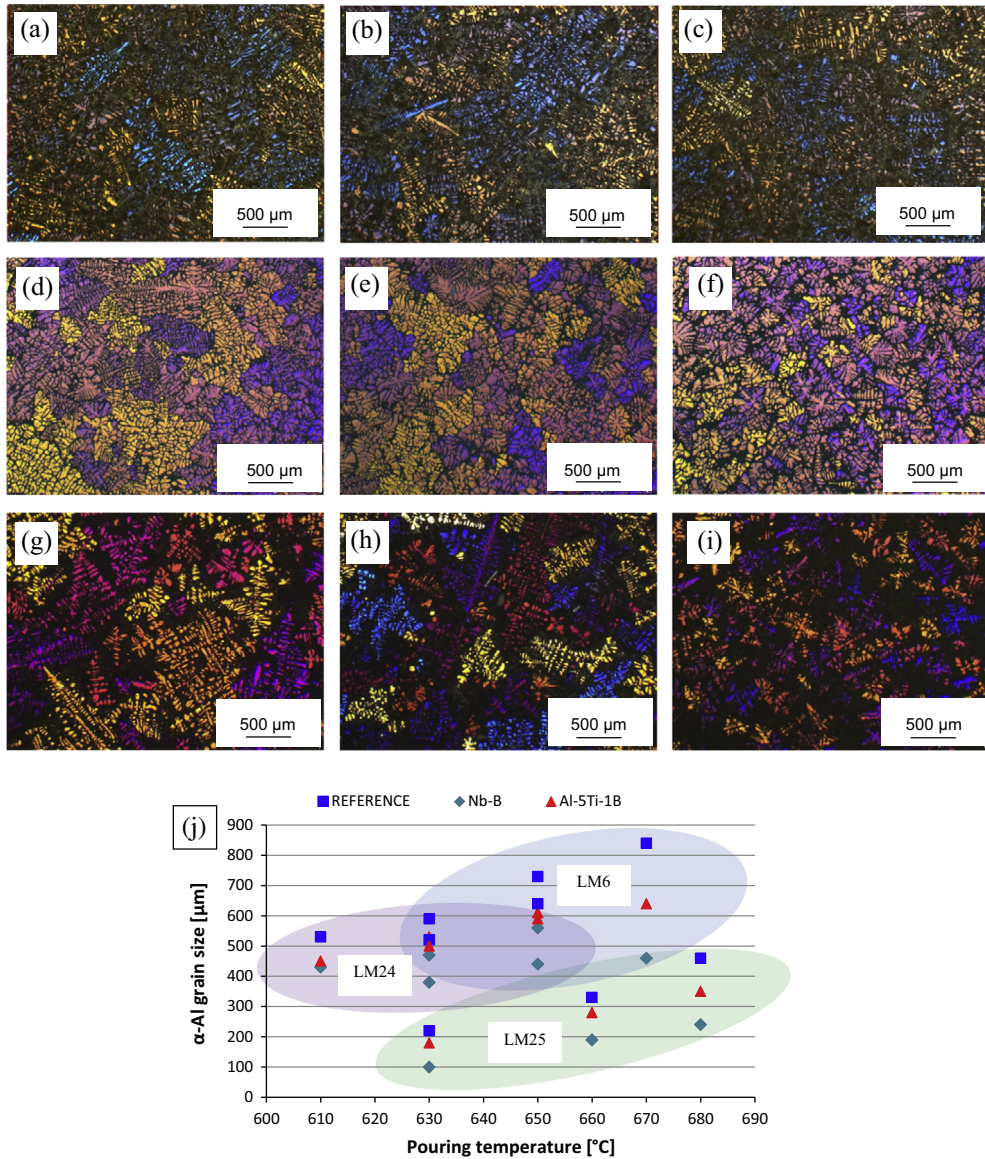


Fig. 1. Micrographs of LM24 alloy samples produced by pouring at 650 $^{\circ}\text{C}$ into TP-1 mould: (a) reference, (b) 0.1 wt.% Al-5Ti-1B and (c) 0.1 wt.% Nb-B; LM25 alloy samples produced by pouring at 680 $^{\circ}\text{C}$ into TP-1 mould: (d) reference, (e) 0.1 wt.% Al-5Ti-1B and (f) 0.1 wt.% Nb-B; LM6 alloy samples produced by pouring at 650 $^{\circ}\text{C}$ into TP-1 mould: (g) reference, (h) 0.1 wt.% Al-5Ti-1B and (i) 0.1 wt.% Nb-B and (j) variation of the grain size with the pouring temperature.

(Fig. 1j). The addition of the commercial Al-5Ti-1B master alloy to the LM25 alloy (Fig. 1e) leads to some refinement of the primary α -Al grain size which is decreased to 180 μm at 630 $^{\circ}\text{C}$ and to 350 μm at 680 $^{\circ}\text{C}$, equivalent to a reduction of almost $19 \pm 4\%$. Moreover, the difference between the reference and the refined materials becomes somewhat more important with the increment of the temperature. Once again, Nb-B inoculation (Fig. 1f) leads to greater refinement of the primary α -Al dendrites with respect to both the untreated alloy and the alloy refined with the commercial Al-5Ti-1B master alloy. Specifically, the final grain size varies from approximately 100 μm to 240 μm or a total grain size reduction of $48 \pm 6\%$. In the case of the LM25 alloy, the performance of the novel Nb-B grain refiner is much better in comparison to the Al-5Ti-1B master alloy than in the LM24 due to the intrinsic growth restriction factors of each single alloying element on α -Al. From the micrograph of the LM6 poured without the addition of any grain refiner (Fig. 1g), the microstructure is composed of relatively large primary α -Al dendrites whose size increases from 520 μm at 630 $^{\circ}\text{C}$ to 840 μm at 670 $^{\circ}\text{C}$ (Fig. 1j). The addition of

the commercial Al-5Ti-1B master alloy (Fig. 1h) does not have any significant effect on the microconstituents of the alloy poured from 630 $^{\circ}\text{C}$ because the grain size is very similar to that of the reference material. With the increment of the solidification temperature, the commercial Al-5Ti-1B master alloy has some beneficial effect for the reduction of the grain size in comparison to the reference and the size of the primary dendrites ranges from 520 μm to 640 μm . Without counting the data of the alloy poured at 630 $^{\circ}\text{C}$, the mean reduction in grain size by the addition of the commercial Al-5Ti-1B master alloy is around $21 \pm 3\%$. As in the case of the LM25 alloy, Nb-B inoculation is much more beneficial for the reduction of the grain size of commercial Al-Si casting alloys already at very low pouring temperature. After the addition of the Nb-B novel grain refiner, the size of the primary α -Al dendrites ranges between 380 μm and 460 μm in solidification ranges studied (630–670 $^{\circ}\text{C}$) equivalent to a mean reduction in grain size of $37 \pm 9\%$. Once again, the effect of the grain refinement becomes more important with the increment of the pouring temperature and the difference with the reference material turns out to be more

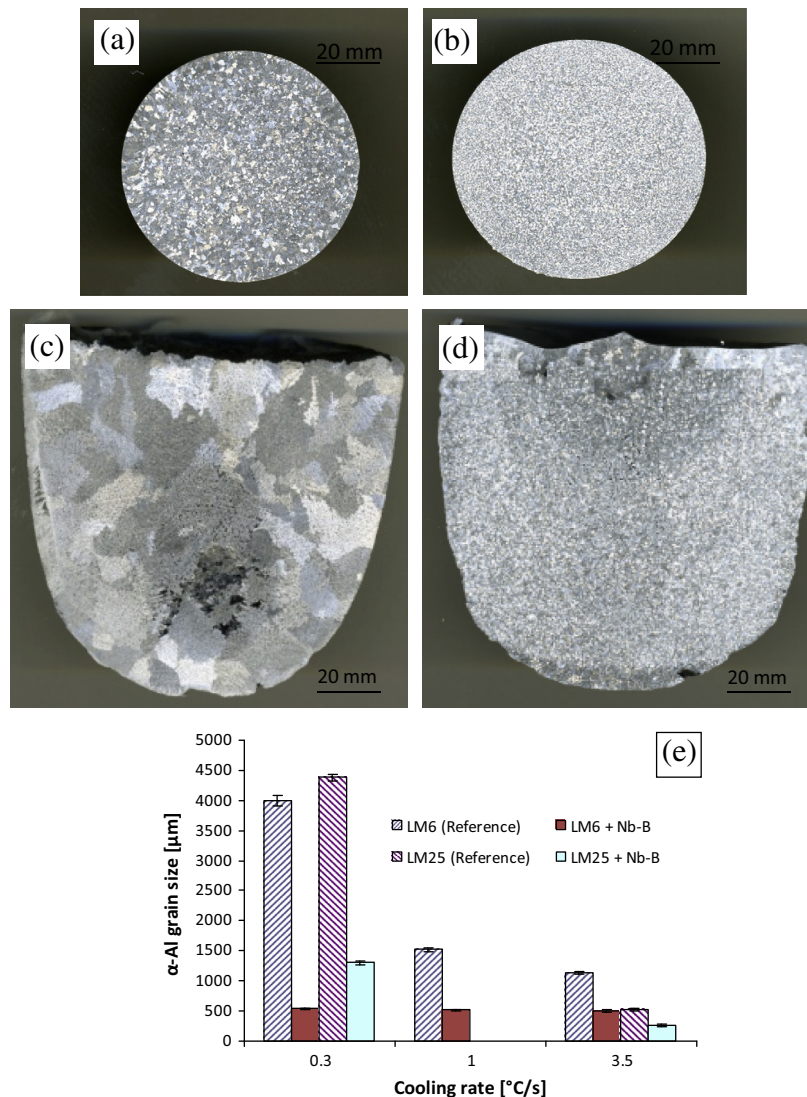


Fig. 2. Macroetched cross-sections of the LM25 alloy (TP-1 mould@700 $^{\circ}\text{C}$): (a) without and (b) with Nb-B inoculation; macroetched cross-sections of the LM6 alloy (slow cooled at 0.3 $^{\circ}\text{C/s}$): (c) without and (d) with Nb-B inoculation, and (e) variation of the grain size with the cooling rate.

obvious. The performance of the novel Nb-B grain refiner in comparison to the commercial Al-5Ti-1B master alloy is kept throughout the whole set of solidification temperatures considered, which are relatively low with respect to the temperature used in the Al industry. Specifically, higher pouring temperatures are needed in Al cast houses in order to guarantee the complete filling of the mould cavities. The difference in terms of efficiency between the commercial and Nb-B inoculation happens to be more significant with the increment of the pouring temperature. This behaviour is expected because at higher processing temperature the poisoning effect [8,20,21] between Ti and Si becomes more pronounced. As explained in Part I of this paper, the efficiency of the novel Nb-B grain refiner is not poisoned because niobium silicides are high temperature intermetallics. Thus, their formation kinetics at temperatures used in Al foundries is much lower in comparison to that of titanium silicides [29].

3.2. Effect of Nb-B inoculation and cooling rate on the microstructure of commercial Al-Si alloys

Fig. 2 shows the effect Nb-B inoculation in the LM25 alloy poured 700 $^{\circ}\text{C}$ into TP-1 mould, LM6 solidified in glass-wool lined crucibles and the variation of the grain size with the cooling rate.

As it can be seen from the macroetched cross-section of the LM25 alloy without the addition of any grain refiner (Fig. 2a), the alloy is characterised by equiaxed primary Al α -grains. The addition of the Nb-B grain refiner permits to obtain a much finer microstructure composed by equiaxed grains. From Fig. 2(e), there is a significant grain coarsening with the decrement of the cooling rate employed to solidify the reference alloys which is not as pronounced after the addition of the Nb-B grain refiner, especially for the LM6 alloy. Therefore, Nb-B inoculation in commercial Al-Si casting alloys with high Si content makes their final grain size less sensitive to the cooling rate. This is very important when casting complex shaped products with different wall thicknesses where the local cooling rate changes depending on the heat extraction which is lower for thicker sections. The extreme difference in terms of grain size between the LM6 alloys prior and after Nb-B inoculation can be clearly seen by comparing the macroetched surface of the samples slow cooled at 0.3 $^{\circ}\text{C/s}$ (Fig. 2c and d). To further verify that Nb-B inoculation potency, LM6 alloy wedge-shaped samples without and with the addition of the Nb-B grain refiner were cast. With this type of configuration the continuous variation of the grain size with the cooling rate can be easily studied. The cooling rate decreases with the widening of the thickness of the samples or, in turns, the decrement of the cooling rate. The

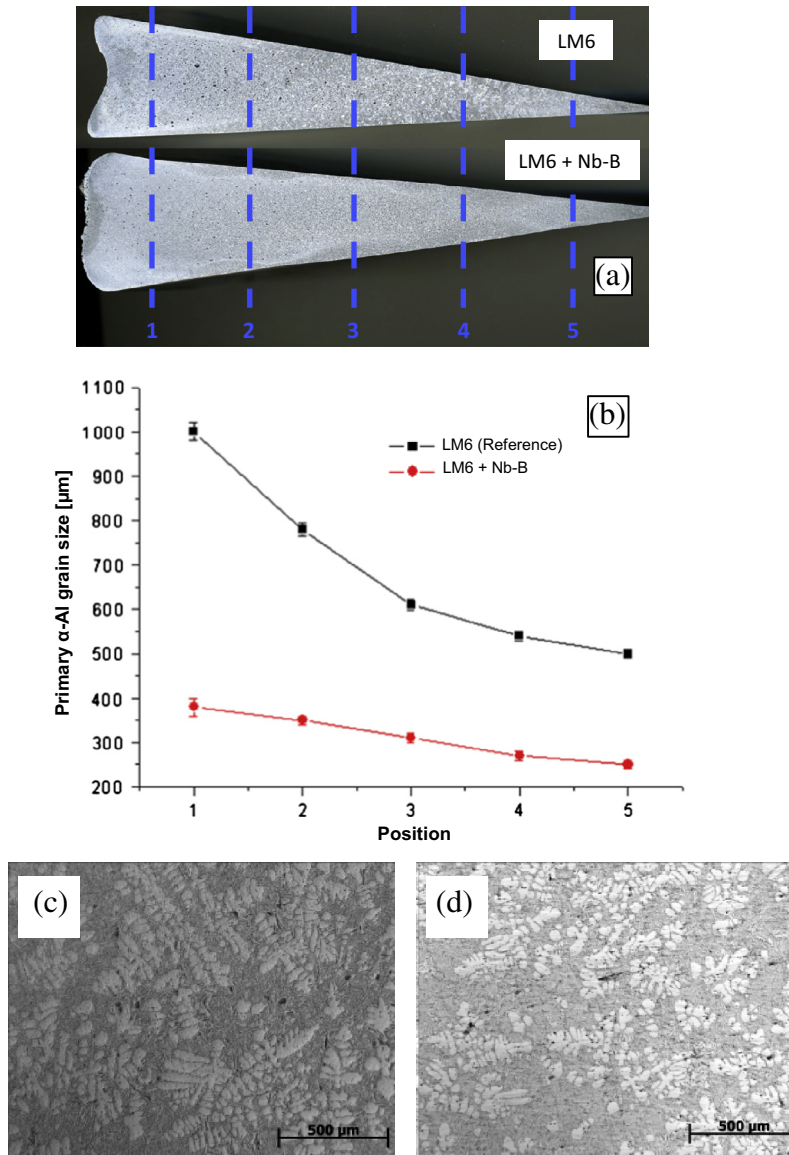


Fig. 3. Effect of fast cooling rate on the grain size of the LM6 alloy: (a) macroetched cross-section of the wedge-shaped samples, (b) variation of the grain size as a function of the position (i.e. cooling rate), (c) microstructure of the reference material (LM6) in position 1, and (d) microstructure of the Nb-B refined material (LM6 + Nb-B) in position 1.

results of these experiments are shown in Fig. 3 where it can be seen that the cooling rate decreases from approximately 90–100 °C/s (position 5), 40–50 °C/s (position 3) to 5–10 °C/s (position 1). Specifically, Fig. 3 displays the macroetched cross-section of the wedge-shaped LM6 samples cast from 740 °C without and with Nb-B inoculation and the variation of the grain size as a function of the position along the length of the specimens.

From their comparison (Fig. 3a), it is already clear that Nb-B inoculation permits to reduce significantly the final size of the primary α -Al dendrites at this quite fast cooling rates. By a closer analysis of the variation of the grain size with the cooling rate (Fig. 3b), the reference material has a relatively small primary α -Al grain size of approximately 500 μm in position 5 (cooling rate of 100 °C/s). With the decrement of the cooling rate, there is an important grain growing reaching a grain size in the order of 1 mm near the slowest cooling rate achievable in the samples (position 1 – cooling rate of 5–10 °C/s). It can be noticed that there is a significant spatial variation of the grain size as a function of the cooling rate and, thus, the final grain size is very dependent on the local cooling rate. After Nb-B inoculation the grain size of the LM6 refined with the grain refiner ranges from 250 μm (position 5) to

380 μm (position 5). Fig. 3(c) and (d) shows representative examples of the microstructure (position 1) of the reference and refined material where the difference in size of the dendritic morphology of the primary α -Al grains can be seen.

In part I of this paper where the effect of the addition of the Nb-B grain refiner to binary Al-xSi alloys was studied, it was found that the inoculation by means of Nb-B significantly refines the size of the primary α -Al dendrites and, as a consequence, a much finer and more homogeneous distribution of the eutectic Al-Si phase is obtained. To double-check that this phenomena is taking place also in commercial Al-Si foundry alloys, the size of the eutectic phase was measured by means of image analysis for the LM6 alloy cooled under different conditions. The results of the variation of the size of the needle-like eutectic phase is presented in Fig. 4 jointly with representative examples of the morphology of this eutectic phase in the LM6 alloy prior and after the addition of the Nb-B grain refiner.

From the results of the variation of the size of the Al-Si eutectic phase shown in Fig. 4(a), it can be seen that the reference material is characterised by a eutectic size of 25–50 μm for cooling rates greater than 2 °C/s. Nevertheless, for very slow cooling rate (i.e. 0.3 °C/s) the length of the needles increases significantly reaching

a mean value of 280 μm . After Nb–B inoculation it can be noticed that the length of the eutectic phase is already smaller in comparison to the reference material over a great cooling rate range 1–100 $^{\circ}\text{C}/\text{s}$, where 100 $^{\circ}\text{C}/\text{s}$ is the underestimated value for HPDC components. Nonetheless, the most drastic reduction of the size of the eutectic is attained at the very slow cooling rate of 0.3 $^{\circ}\text{C}/\text{s}$ where the eutectic size is reduced from 280 μm to 130 μm . This achievement is very important because under this low cooling rate conditions is also very difficult to obtain the “modification” of the needle-like eutectic phase to a fibrous morphology by strontium addition [30,31]. Consequently, the achievement of fine eutectic needles by grain refinement is highly advantageous. The much greater amount of smaller Al–Si eutectic particles obtained after Nb–B inoculation can be seen by comparing Fig. 4(c) with Fig. 4(b). It is worth mentioning that, no new phases (such as intermetallics) from the interaction of the Nb–B inoculants and the alloying elements of the Al–Si alloys were found during the microstructural analysis.

3.3. Effect of Nb–B inoculation on the mechanical properties of commercial Al–Si alloys

Tensile data and hardness measurements [32] are reported in Fig. 5(a) and (b), respectively.

From Fig. 5(a), it can be seen that the grain refinement of the LM25 and LM6 alloys by means of the Nb–B grain refiner leads to the increment of the ultimate tensile strength. Moreover, the materials show better ductility which is especially visible for the LM6 alloy. These improvements are due to the finer primary α -Al dendrites and finer Al–Si eutectic found after the addition of the Nb–B grain refiner. Moreover, because of the more homogeneous distribution of the alloying elements (especially Si) during solidification and the greater number of grain growing, less microporosity is present in the material. The LM25 alloy is commonly subjected

to heat treatments of solubilisation and ageing known as T6 (solution plus artificial ageing) or T7 (solution plus stabilising) [3]. In this case, the effect of the TB7 heat treatment (solution treatment and stabilisation at 532 $^{\circ}\text{C}$ during 5 h plus hot water quenching and ageing at 250 $^{\circ}\text{C}$ during 3 h) on the LM25 alloy without and with Nb–B inoculation was also considered. The results of the tensile tests performed on the heat treated LM25 alloy show that this heat treatment induces an increment of the ductility which is further significantly enhanced by the inoculation of the alloy prior heat treatment. From the results of the tensile test performed on the LM24 alloy tensile samples produced by HPDC (Fig. 5), it can be seen that the addition of the Nb–B grain refiner leads to some improvement of the ductility of the material but not of the strength. In the case of HPDC products, Nb–B inoculation does not increase the strength because the material is already characterised by very fine microstructures due to the extremely high cooling rate intrinsic of the injection process. In the case of the elongation, the improvement induced by the addition of the Nb–B grain refiner is due to the reduce size of the externally solidified crystals (ESC), solidification of equiaxed grains which takes place when the alloy is poured into the shot sleeve, and the reduction of the defect bands. Specifically, this defect band is a typical feature of HPDC products and it is normally constituted of ESCs, porosity and solidified phases with very high solute concentrated (i.e. Si) due to segregation phenomena [33]. By analysing the data of the Vickers hardness measurements (Fig. 5b), it can be noticed that the hardness of the reference LM6 alloy increases along with the cooling rate, the typical behaviour for metals due to reduction of the grain size. In the case of the addition of the novel Nb–B grain refiner, the refined alloy always shows higher hardness and the improvement with respect to the reference material is much more noticeable at lower cooling rate where the difference in terms of microstructural features is significantly bigger.

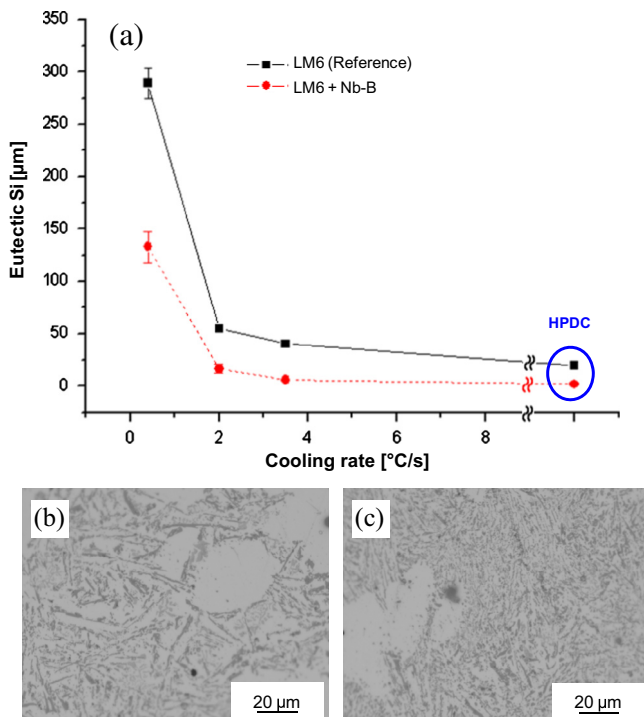


Fig. 4. Details of the Al–Si eutectic phase of the LM6 alloy: (a) variation of the needle-like eutectic phase with the cooling rate, (b) micrograph showing the eutectic morphology of the LM6 reference alloy (TP-1 mould), and (c) micrograph showing the eutectic morphology of the Nb–B grain refined LM6 alloy (TP-1 mould).

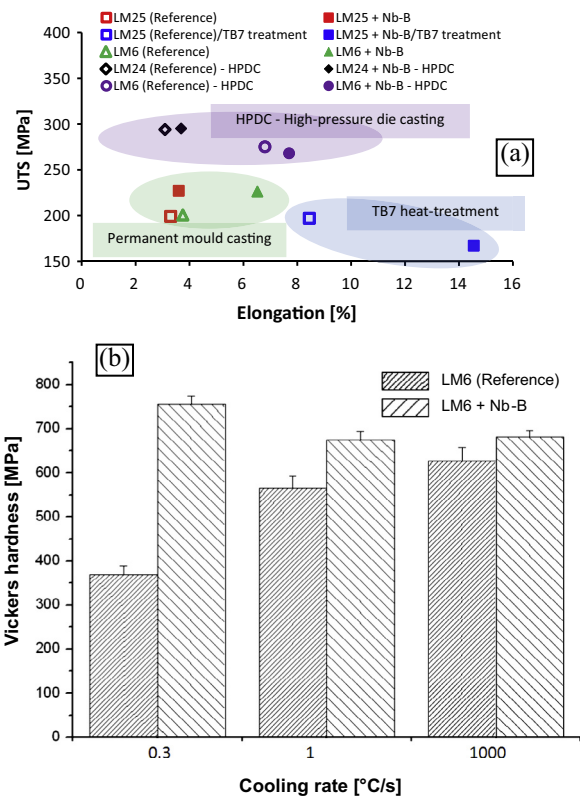


Fig. 5. Mechanical properties of the commercial Al–Si alloys without and with Nb–B inoculation [32]: (a) ultimate tensile strength vs. elongation, and (b) Vickers hardness.

3.4. Identification of the heterogeneous nucleation sites and effect on undercooling

In order to identify the nucleants added to the melt by the addition of the Nb–B powders which are responsible for the grain refinement, pure Al after the addition of 0.1 wt.% of Nb and KBF_4 powders was analysed by SEM. Fig. 6 shows the morphology of the intermetallic particles found in the α -Al grains with the EDS (energy-dispersive spectroscopy) spectra of the Al_3Nb particles found.

From the SEM analysis it is found that the three elements (Al, Nb and B) react to form different compounds such as niobium aluminides (Al_3Nb) and niobium borides (i.e. NbB_2). These Nb-based compounds are the potential heterogeneous nucleation substrates (i.e. inoculants) which promotes the grain refinement of Al–Si alloys via heterogeneous nucleation.

Thermal analysis was used in order to confirm the presence and activity of the inoculants prior to the nucleation of the α -Al grains. Precisely, the solidification behaviour of the LM6 alloy (macro-etched cross-sections shown in Fig. 2) was studied by means of thermal analysis because this technique is able to determine the efficiency of grain refiners [6]. The cooling curves of the LM6 without and with Nb–B inoculation were recorded using the NI-VI Logger dedicated data software to collect 100 data/s. From the cooling curves, the nucleation, minimum and growth temperatures and the undercooling (ΔT) are calculated. The plot of the cooling curves and the characteristic temperatures are reported in Fig. 7 and Table 2, respectively.

From the results of the differential thermal analysis (Fig. 7 and Table 2), the nucleation temperature, point from which the primary α -Al crystals nucleate and agglomerate into clusters which are stable to growth, is around 590 °C for the LM6 alloy and this temperature is slightly higher after the addition of the Nb–B grain refiner.

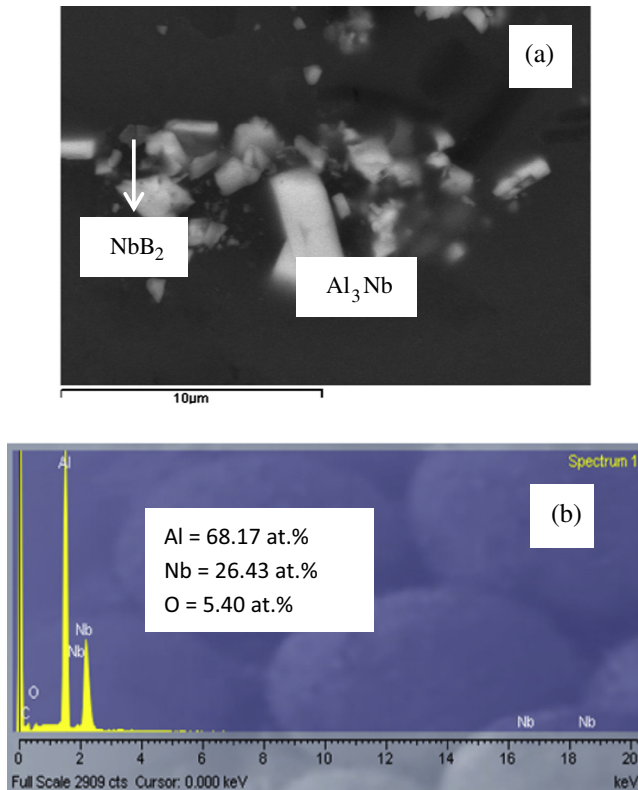


Fig. 6. SEM micrograph of the intermetallic particles in Al by the addition of 0.1 wt.% Nb and B powder (a) and EDS spectra of the Al_3Nb intermetallics (b).

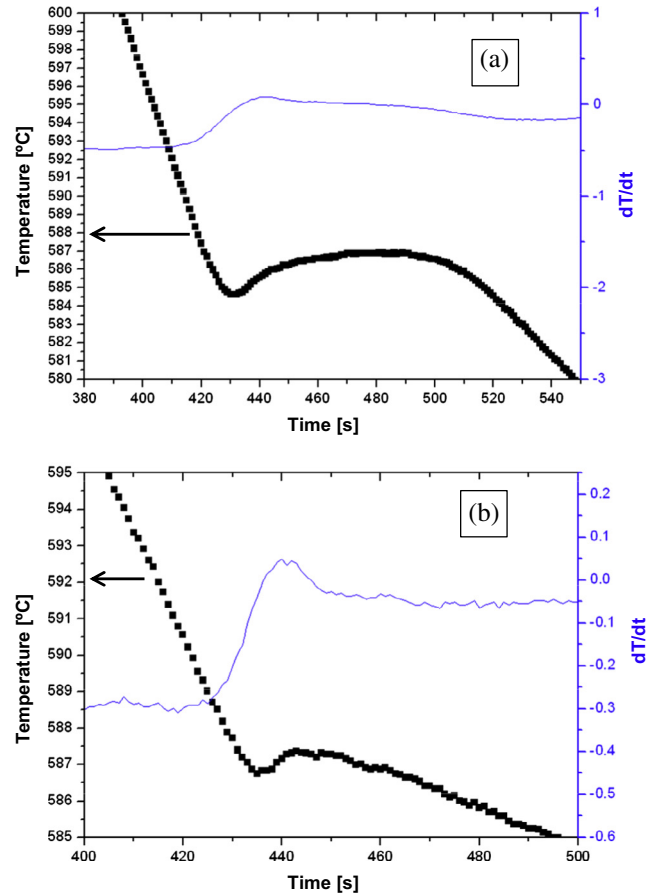


Fig. 7. Comparison of the cooling curves of the commercial LM6 alloy: (a) without, and (b) with Nb–B inoculation.

Table 2

Primary α -Al temperature (T_N), minimum temperature (T_{min}), growth temperature (T_G) and undercooling for primary α -Al nucleation (ΔT) determined from the cooling curves displayed in Fig. 7.

		T_N (°C)	T_{min} (°C)	T_G (°C)	ΔT (°C)
LM6 alloy	Reference	588.3	584.5	587.0	2.5
	Nb–B inoculation	588.8	586.8	587.5	0.7

During thermal analysis only the primary α -Al and eutectic nucleation reactions were detected. Another confirmation that the Nb–B inoculants are chemical stable in commercial Al–Si alloys and do not form reaction products. The undercooling results to be 2.5 °C in the case of the reference material and 0.7 °C after the addition of the Nb–B grain refiner. The reduction of the undercooling is a further evidence that Nb–B inoculation induces heterogeneous nucleation. This is because an ideal heterogeneous nucleation site would have nucleation energy equal to zero. From this, the efficiency of a grain refiner is indirectly correlated to the undercooling [6]. The experimental result presented indicates that Al–Si casting alloys are effectively refined by the Nb–B grain refiner with an undercooling of 0.7 °C (Table 2). The low undercooling suggests that the lattice mismatch between the Nb–B inoculants and the α -Al nucleating phase is very small.

4. Conclusions

The general conclusion that can be drawn from this study is that the addition of the Nb–B grain refiner can efficiently and reliably

refine the microstructural features of Al–Si cast alloys. No interaction between the Nb–B inoculants and the alloying elements of commercial Al–Si alloys was found confirming the chemical stability of the Nb-based compounds. The main effect of Nb–B inoculation in Al–Si alloy is seen in the refinement of the size of the primary α -Al dendrites although there is a refinement of the Al–Si eutectic phase. Moreover, Nb–B inoculation makes the final grain size of the Al–Si alloy less dependent on the cooling rate which indicates that it could be applied for different casting processes (i.e. sand casting, permanent mould casting and pressure casting). Another effect produced by Nb–B inoculation is the reduction of the undercooling for the nucleation of the primary α -Al dendrites. Finally, the smaller grain size obtained after Nb–B inoculation, normally, leads to some improvement of the mechanical performances of the Al–Si alloy although they still greatly depend on the production process (i.e. casting method, heat-treatment, etc.). The Al_3Nb and NbB_2 in-situ formed intermetallic particles are the inoculants responsible for the heterogeneous nucleation of α -Al grains. The heterogeneous nucleation mechanism is confirmed by the reduction of the undercooling after Nb–B inoculation detected by thermal analysis.

Acknowledgements

The authors are thankful for the financial support from the Technology Strategy Board (TSB) through the TSB/101177 Project and to the Engineering and Physical Sciences Research Council (EPSRC) through the EP/J013749/1 Project.

References

- [1] Polmear IJ. *Light alloys. Metallurgy of the light metals*. 2nd ed. Edward Arnold; 1989.
- [2] Kutz M. *Mechanical engineers handbook: materials and mechanical design*. 3rd ed. New jersey: John Wiley & Sons; 2005.
- [3] Davis JR. *ASM speciality handbook: aluminum and aluminum alloys*. Ohio: ASM International Light Alloys; 1993.
- [4] Rooy EL. *Aluminum and aluminum alloys*. Castings, vol. 15. Ohio: ASM International; 1988.
- [5] McCartney DG. Grain refining of aluminium and its alloys using inoculants. *Int Mater Rev* 1989;34:247–60.
- [6] Murty BS, Kori SA, Chakraborty M. Grain refinement of aluminium and its alloys by heterogeneous nucleation and alloying. *Int Mater Rev* 2002;47:3–29.
- [7] Sigworth GK. The grain refining of aluminum and phase relationships in the Al–Ti–B system. *Metall Trans A* 1984;15:277–82.
- [8] Sigworth GK, Guzowski MM. Grain refining of hypoeutectic Al–Si alloys. *AFS Transactions* 1985;93:907–12.
- [9] Guzowski MM, Sigworth GK, Sentner DA. The role of boron in the grain refinement of aluminum with titanium. *Metall Trans A* 1987;18:603–19.
- [10] Sritharan T, Li H. Influence of titanium to boron ratio on the ability to grain refine aluminium–silicon alloys. *J Mater Process Technol* 1997;63:585–9.
- [11] Greer AL, Cooper PS, Meredith MW, Schneider W, Schumacher P, Spittle JA, et al. Grain refinement of aluminium alloys by inoculation. *Adv Eng Mater* 2003;5:81–91.
- [12] Nafisi S, Ghomashchi R. Grain refining of conventional and semi-solid A356 Al–Si alloy. *J Mater Process Technol* 2006;174:371–83.
- [13] Zhang Y, Ma N, Wang H, Li X. Study on damping behavior of A356 alloy after grain refinement. *Mater Des* 2008;29:706–8.
- [14] Gezer BT, Toptan F, Daglilar S, Kerti I. Production of Al–Ti–C grain refiners with the addition of elemental carbon. *Mater Des* 2010;31:S30–5.
- [15] Shabani MJ, Emamy M, Nemati N. Effect of grain refinement on the microstructure and tensile properties of thin 319 Al castings. *Mater Des* 2011;32:1542–7.
- [16] Li P, Liu S, Zhang L, Liu X. Grain refinement of A356 alloy by Al–Ti–B–C master alloy and its effect on mechanical properties. *Mater Des* 2013;47:522–8.
- [17] Samuel E, Golbahar B, Samuel AM, Doty HW, Valtierra S, Samuel FH. Effect of grain refiner on the tensile and impact properties of Al–Si–Mg cast alloys. *Mater Des* 2014;56:468–79.
- [18] Spittle JA, Sadli S. Effect of alloy variables on grain refinement of binary aluminium alloys with Al–Ti–B. *Mater Sci Technol* 1995;11:533–7.
- [19] Spittle JA, Keeble JM, Meshhedani AL. The grain refinement of Al–Si foundry alloys. *Light Metals* 1997;795–800.
- [20] Mohanty PS, Gruzleski JE. Grain refinement mechanisms of hypoeutectic Al–Si alloys. *Acta Materialia* 1996;44:3749–60.
- [21] Kori SA, Auradi V, Murty BS, Chakraborty M. Poisoning and fading mechanism of grain refinement in Al–7Si alloy. *Mater Forum* 2005;29:387–93.
- [22] Cooper PS, Hardman A, Boot D, Burhop E. Characterisation of a new generation of grain refiners for the foundry industry. *Light Metals* 2003.
- [23] Polmear IJ. *Light alloys. From traditional alloys to nanocrystals*. 4th ed. UK: Butterworth-Heinemann; 2006.
- [24] The Aluminum Association. TP-1 – Standard Test Procedure for Aluminum Alloy Grain Refiners. 2002:Washington DC, USA.
- [25] Johnsson M, Bäckkerud L. The influence of composition on equiaxed crystal growth mechanisms and grain size in Al alloys. *Zeitschrift für Metallkunde* 1994;85:781–5.
- [26] Knuutinen A, Nogita K, McDonald SD, Dahle AK. Modification of Al–Si alloys with Ba, Ca, Y and Yb. *J Light Metals* 2001;1:229–40.
- [27] Apelian D, Sigworth GK, Whaler KR. Assessment of grain refinement and modification of Al–Si foundry alloys by thermal analysis. *AFS Transactions* 1984;92:297–307.
- [28] Das A, Kotadia HR. Effect of high-intensity ultrasonic irradiation on the modification of solidification microstructure in a Si-rich hypoeutectic Al–Si alloy. *Mater Chem Phys* 2011;125:853–9.
- [29] Zhao JC, Jackson MR, Peluso LA. Mapping of the Nb–Ti–Si phase diagram using diffusion multiples. *Mater Sci Eng A* 2004;372:21–7.
- [30] Hengcheng L, Juanjuan B, Min Z, Ke D, Yunfeng J, Ingdong C. Effect of strontium and solidification rate on eutectic grain structure in an Al-13 wt% Si Alloy. *China Foundry* 2009;6:226–31.
- [31] Sun S-C, Yuan B, Liu M-P. Effects of moulding sands and wall thickness on microstructure and mechanical properties of Sr-modified A356 aluminum casting alloy. *Trans Nonferrous Metals Soc China* 2012;22:1884–90.
- [32] Nowak M. Development of Niobium-Boron Grain Refiner for Aluminium-Silicon Alloys. Ph.D. Thesis, Brunel University, London (U.K.), 2011, <<http://bura.brunel.ac.uk/handle/2438/8321>> [accessed: .07.14].
- [33] Dahle AK, StJohn DH. Rheological behaviour of the mushy zone and its effect on the formation of casting defects during solidification. *Acta Materialia* 1998;47:31–41.